CrystEngComm

Dynamic Article Links

Cite this: *CrystEngComm*, 2012, **14**, 460

www.rsc.org/crystengcomm

PAPER

Structural phase transition in the β″-(BEDT-TTF)$_4$H$_3$O[Fe(C$_2$O$_4$)$_3$]·G crystals (where G is a guest solvent molecule)†

Leokadiya V. Zorina,*[a] Salavat S. Khasanov,[a] Sergey V. Simonov,[a] Rimma P. Shibaeva,[a] Pavlo O. Bulanchuk,[ab] Vladimir N. Zverev,[a] Enric Canadell,[c] Tatiana G. Prokhorova[d] and Eduard B. Yagubskii[d]

Received 13th July 2011, Accepted 22nd September 2011
DOI: 10.1039/c1ce05878a

A structural phase transition from monoclinic *C*2/*c* to triclinic *P*$\bar{1}$ symmetry has been found by X-ray diffraction in a number of single crystals of the known family of organic metals and superconductors β″-(BEDT-TTF)$_4$H$_3$O[Fe(C$_2$O$_4$)$_3$]·G where G stands for halogenated benzene derivatives and their mixtures with benzonitrile. The transition occurs upon lowering the temperature at 180–230 K. Comparison of the crystal and electronic structure of the monoclinic and triclinic phases reveals details of the structural transformations in the (PhCl + PhCN)-containing superconducting β″-crystal, as an example. It is shown that the transition concerns mainly the anion layer and has a weak influence on the structure of the BEDT-TTF layer and, consequently, on the conducting properties of the single crystals.

Introduction

Recently, we have performed an intensive study of the well-known (BEDT-TTF)$_4$(H$_3$O)$^+$[Fe^{III}(C$_2$O$_4$)$_3$]·G family of organic conductors and superconductors. In particular, a modified procedure of the electrochemical synthesis was proposed,[1] which allowed to obtain a large number of crystals of this family containing different solvents and their mixtures, with β″, 'pseudo-κ' and novel α-'pseudo-κ' packing of the conducting BEDT-TTF layers. This family has been investigated since 1995[2] and today it involves four polymorphic phases of the same stoichiometry (including α-β″ phase[3,4] in addition to the listed above). Two of four phases have a bi-layered structure with different packing of the alternating organic donor layers, which is a unique case for organic conductors. Crystals of the β″-phase form the largest group in the family and are extensively studied due to their superconducting properties.[1,2,5–9] Similarities and distinctions in the arrangement of the anion and donor layers in all four phases have been illustrated in our recent article.[10]

Remarkably, the formation of a certain phase is essentially determined by the size, symmetry and composition of the neutral solvent molecule which enters as a guest into the large hexagonal cavities of the anion layer. It was also shown that the solvent nature has a significant influence on the superconductivity of the β″-crystals.[11–17] The degree of positional ordering of the terminal ethylene groups in the BEDT-TTF molecules and T_c directly depends on the solvent size. All β″-phases are disordered at room temperature, and a superconducting transition takes place only if a donor ordering occurs upon temperature decrease. Note, that the process of the atomic ordering in BEDT-TTF does not destroy the monoclinic *C*2/*c* symmetry of the β″-crystals.

We have performed an X-ray study at different temperatures of a large series of β″-(BEDT-TTF)$_4$H$_3$O[Fe(C$_2$O$_4$)$_3$]·G crystals with different solvents and their mixtures. In a number of them [G = FB, CB, (BN)$_{0.40}$(FB)$_{0.60}$, (BN)$_{0.35}$(CB)$_{0.65}$, (BN)$_{0.17}$(BB)$_{0.83}$, where FB is fluorobenzene, CB is chlorobenzene, BB is bromobenzene, BN is benzonitrile] a structural phase transition from monoclinic to triclinic symmetry has been discovered. Similar transition was mentioned only once for the superconducting crystal with G = BB[18] but with no further structural investigation, though it was confirmed by heat capacity measurements. The origin of the transition, crystal and electronic structures above and below the phase transition temperature (studied for the case of a (BN)$_{0.35}$(CB)$_{0.65}$-containing crystal) as well as the effect of the structural transition onto the conducting properties of the crystals are discussed in the present article.

Experimental

X-ray diffraction

The single crystal X-ray structural study was carried out using an Oxford Diffraction Gemini-R diffractometer [λ(Mo-Kα) = 0.71073 Å, graphite monochromator, Ruby CCD detector]. Nine β″-(BEDT-TTF)$_4$H$_3$O[Fe(C$_2$O$_4$)$_3$]·G crystals with different

[a]*Institute of Solid State Physics, RAS, Chernogolovka, MD, 142432, Russia. E-mail: zorina@issp.ac.ru*
[b]*Moscow Institute of Physics and Technology, Dolgoprudny, Moscow region, Russia*
[c]*Institut de Ciència de Materials de Barcelona, CSIC, Campus de la UAB, E-08193 Bellaterra, Spain*
[d]*Institute of Problems of Chemical Physics, RAS, Chernogolovka, MD, 142432, Russia*

† Electronic supplementary information (ESI) available. CCDC reference numbers 771736 and 833651. For ESI and crystallographic data in CIF or other electronic format see DOI: 10.1039/c1ce05878a

solvent molecules G were investigated in 300–100 K range with the aim to check temperature stability of the crystal structure (full list of the compounds is given in the beginning of the Results and Discussion section, their synthesis and room temperature structures were reported earlier[1]). Four of them keep monoclinic symmetry of the room temperature state down to 100 K while in the other five compounds, structural phase transition to triclinic symmetry has been identified between 180 and 230 K. The temperature of the transition was detected by appearance of the additional diffraction reflections on X-ray rotation images which were made with 3–5 degree steps. For all the crystals full data collections were performed above and below the transition temperature. Corresponding unit cell parameters in the triclinic state and experimental (*h*0*l*) reciprocal-lattice planes illustrating the symmetry lowering are given in the ESI.† The integration of the experimental intensities was hampered by appearance of twinning in the low temperature triclinic phase with small angle of discrepancy of two twin lattices. The best structure refinement results were obtained for β″-(BEDT-TTF)$_4$H$_3$O[Fe(C$_2$O$_4$)$_3$](BN)$_{0.35}$(CB)$_{0.65}$ crystal and used for the detailed structure analysis although all five crystals show similar structural changes in the course of the transition.

For the β″-(BEDT-TTF)$_4$H$_3$O[Fe(C$_2$O$_4$)$_3$](BN)$_{0.35}$(CB)$_{0.65}$ crystal experimental data sets were collected at room temperature and 150 K using ω-scan procedure. Data reduction with empirical absorption correction of experimental intensities (Scale3AbsPack program) was made with the CrysAlisPro software.[19]

The structure was solved by a direct method followed by Fourier syntheses and refined by a full-matrix least-squares method using the SHELX-97 programs[20] in an anisotropic approximation for all non-hydrogen atoms. H-atoms in BEDT-TTF and solvent molecules were placed in idealized positions and refined using a riding model, U_{iso}(H) were fixed at 1.2U_{eq}(C). Coordinates of the H-atoms in the hydroxonium H_3O^+ cations were found from difference electron density map and refined with U_{iso}(H) = 1.5U_{eq}(O), O–H bond lengths were restrained to equal value with standard deviation of 0.02 Å (SADI instruction).

Crystal data. C$_{52.35}$H$_{40}$Cl$_{0.65}$FeN$_{0.35}$O$_{13}$S$_{32}$, M = 1986.76, T = 150(1)K, triclinic, a = 10.2649(3), b = 11.1956(3), c = 35.1514 (10) Å, α = 88.619(2), β = 86.651(2), γ = 62.748(3)°, V = 3585.1 (2) Å^3, $P\bar{1}$, Z = 2, D_c = 1.840 g cm^{-3}, μ = 12.28 cm^{-1}, $2\Theta_{max}$ = 65.98°, reflections measured 45485, unique reflections 23141 (R_{int} = 0.0332), reflections with $I > 2\sigma(I)$ = 19179, parameters refined 987, R_1 = 0.0519, wR_2 = 0.1251, GOF = 1.010. Unit cell parameters at 293 K are: monoclinic, a = 10.2763(6), b = 20.067 (1), c = 35.369(2) Å, β = 92.915(6)°, V = 7284.2(7) Å^3, $C2/c$, Z = 4; R_1 = 0.0390. Crystallographic data for the 293 K structure have been published earlier.[1]

Electronic band structure calculations

The tight-binding band structure calculations[21] were of the extended Hückel type. A modified Wolfsberg-Helmholtz formula was used to calculate the non-diagonal $H_{\mu\nu}$ values.[22] All valence electrons were taken into account in the calculations and the basis set consisted of Slater-type orbitals of double-ζ quality for C 2s and 2p, S 3s and 3p and of single-ζ quality for H. The ionization potentials, contraction coefficients and exponents were taken from previous work.[23]

Conductivity measurements

The temperature dependence of the electrical resistance of single crystal was measured using a four-probe technique by a lock-in detector at 20 Hz alternating current J = 1 mkA. Two contacts were attached to each of two opposite sample surfaces with conducting graphite paste. In the experiment we have measured the out-of-plane resistance $R_\perp$ with the current running perpendicular to conducting layers. The temperature sweeping rate did not exceed 2 K min^{-1} for both up and down directions.

Results and discussion

Crystal structure

A series of single crystals of the β″-(BEDT-TTF)$_4$H$_3$O[Fe(C$_2$O$_4$)$_3$]·G family with different guest solvent molecules G: BN, FB, CB, 1,2-DCB (DCB—dichlorobenzene) and mixed (BN)$_{0.86}$(DCB)$_{0.14}$, (BN)$_{0.8}$(NB)$_{0.2}$ (NB—nitrobenzene), (BN)$_{0.40}$(FB)$_{0.60}$, (BN)$_{0.35}$(CB)$_{0.65}$, (BN)$_{0.17}$(BB)$_{0.83}$ has been studied by X-ray diffraction at different temperatures. A structural phase transition was found in five salts with G = FB, CB and a mixture of FB, CB, BB with BN (see ESI†). Crystals with FB or CB exhibit metallic properties down to liquid helium temperature while crystals with mixed solvents are superconductors with T_c = 6.0 K for G = (BN)$_{0.40}$(FB)$_{0.60}$ and (BN)$_{0.35}$(CB)$_{0.65}$ and 4.2 K for (BN)$_{0.17}$(BB)$_{0.83}$.[1] Here a detailed structural analysis of the transition is made for the example of a superconducting β″-(BEDT-TTF)$_4$H$_3$O[Fe(C$_2$O$_4$)$_3$](BN)$_{0.35}$(CB)$_{0.65}$ crystal in the room temperature monoclinic state and in the 150 K triclinic state.

The transition occurs upon lowering the temperature at 180–230 K (depending on the solvent composition) and is accompanied by a lowering of the symmetry from monoclinic $C2/c$ to triclinic $P\bar{1}$. Appearance of the additional diffraction reflections below the phase transition point (Fig. 1b and Fig. 1 in ESI†) reveals vanishing of the systematic absences of the monoclinic $C2/c$ lattice. Besides, splitting of the reflections in the (0*kl*) planes (Fig. 1d) indicates weak distortion and twinning of the lattice. In the triclinic phase the crystal becomes twinned by a two-fold rotation around the former monoclinic axis. The refined twin fraction for the β″-(BEDT-TTF)$_4$H$_3$O[Fe(C$_2$O$_4$)$_3$](BN)$_{0.35}$(CB)$_{0.65}$ crystal is 0.3675(9).

A projection of the triclinic structure at 150 K along the *a*-direction is shown in Fig. 2. The structure consists of conducting organic BEDT-TTF layers separated by complex anion layers {(H$_3$O)$^+$[Fe(C$_2$O$_4$)$_3$]$^{3-}$(BN)$_{0.35}$(CB)$_{0.65}$}$^{2-}$ along *c*. Fe^{3+} and H_3O^+ cations are connected by oxalate bridges and form a honeycomb-like network (Fig. 3). The hexagonal cavities of the anion layer are filled by solvent BN and CB molecules in stochastic order.

At room temperature all components of the anion layer are located on 2-fold monoclinic axis; the anion and BN solvent are completely ordered, while the CB solvent and H_3O are slightly disordered relative to the axis. The donor layer contains two independent BEDT-TTF donors in general positions. Both terminal ethylene groups of one BEDT-TTF are disordered between two sites with 0.74/0.26 and 0.75/0.25 occupancies while the second BEDT-TTF is completely ordered already at room temperature (the latter is typical for all known β″-crystals).

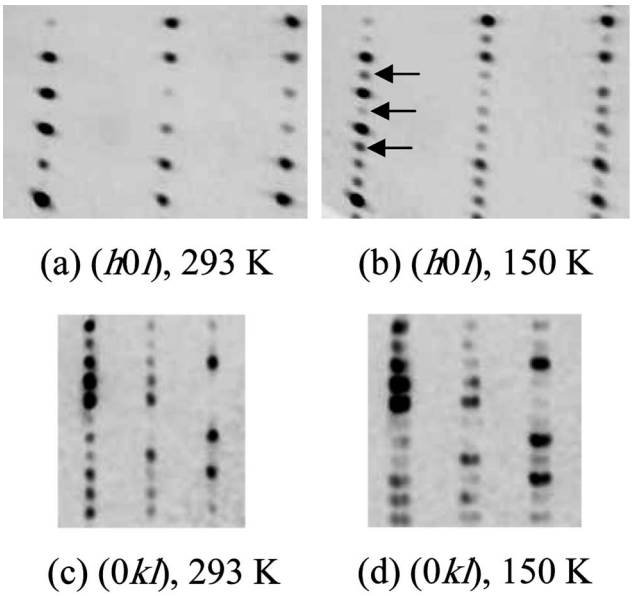

Fig. 1 Fragments of reciprocal-lattice planes calculated on the basis of experimental X-ray data at 293 K (a, c) and 150 K (b, d). (*h*0*l*) (a, b): appearance of additional diffraction reflections with $l \neq 2n$ below the phase transition temperature (shown by arrows in b) destroying the *c*-plane of the monoclinic lattice. (0*kl*) (c, d): triclinic distortion of the lattice with twinning (split reflections in d).

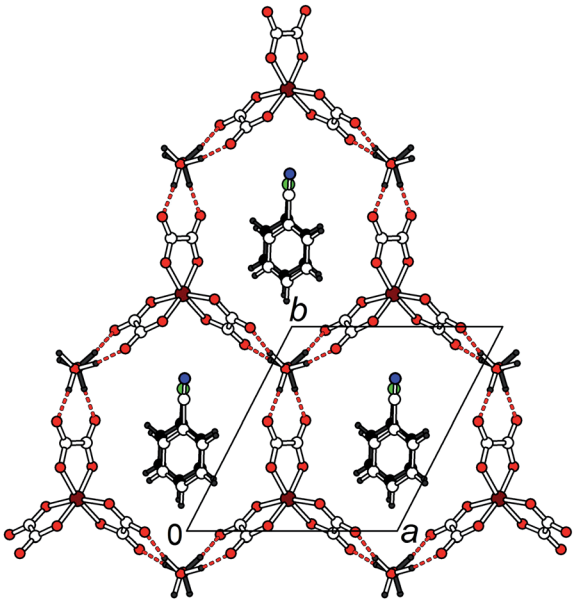

Fig. 3 Projection of the complex honeycomb-like anion layer $\{(H_3O)^+[Fe(C_2O_4)_3]^{3-}(BN)_{0.35}(CB)_{0.65}\}^{2-}$ along *c* in the triclinic structure at 150 K. Two positions of mixed solvent and disordered H_3O^+ cation are shown by white and black colors. Hydrogen contacts are shown by dashed red lines.

As it was mentioned in the Introduction, the ordering of the BEDT-TTF molecules is extremely important for the occurrence of superconductivity in the β″-salts of the family. The superconducting transition is observed in the salts where positional ordering of the ethylene groups occurs under temperature lowering. In the $P\bar{1}$ structure two donor layers become nonequivalent. The triclinic unit cell contains four independent donors, I–IV, two in each layer. Two BEDT-TTF donors (II and III in Fig. 2) are completely ordered in agreement with the room temperature monoclinic structure. A partial ordering occurs in the other two donors (I and IV): at 150 K only one terminal ethylene group is ordered, while for the second one two sites with 0.60/0.40 (in I) and 0.62/0.38 (in IV) occupancies are still observed. With the aim to determine the role of donor ordering in the phase transition process, additional short X-ray diffraction experiments were performed at 190 and 100 K. It was found that, in the triclinic structure at 190 K, *i.e.*, just below the phase transition point, there is no additional ordering in the BEDT-TTF molecules as compared to the monoclinic structure while at 100 K the BEDT-TTF layer is already fully ordered. Two processes seem to go independently in the crystal and are slightly separated in the temperature scale: the first, dramatic structural transformation with the change of symmetry is followed by a classical for organic conductors smooth disorder-

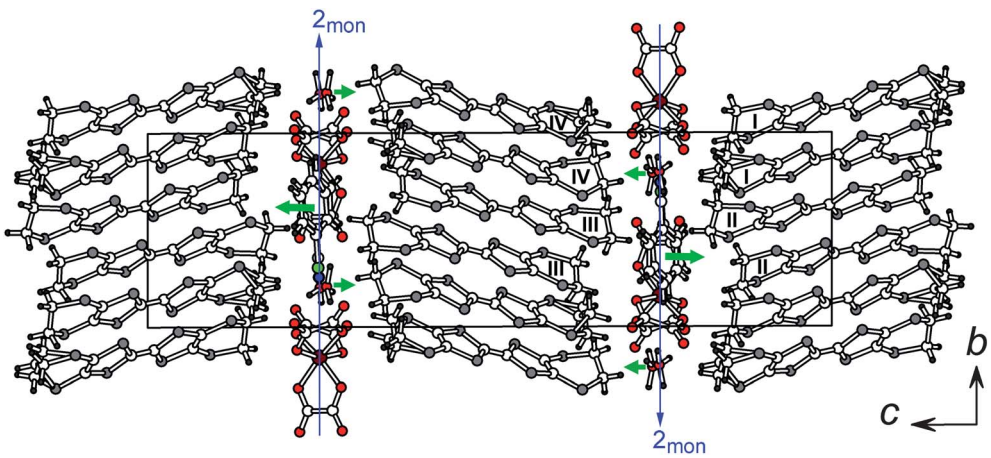

Fig. 2 β″-$(BEDT\text{-}TTF)_4H_3O[Fe(C_2O_4)_3](BN)_{0.35}(CB)_{0.65}$, 150 K: projection of the triclinic structure along *a*. Four independent BEDT-TTF donors are marked by Roman numerals I–IV. Thin blue arrows indicate the position of the monoclinic axis (2_{mon}) in the high-temperature *C*2/*c* phase. Thick green arrows show the direction of shift of the solvent molecules and H_3O^+ ions from the virtual monoclinic axis.

order transition in the organic donor layer under further cooling. It is significant, that the monoclinic to triclinic phase transition does not prevent the important ordering process in the superconducting crystal. As the $C2/c$ to $P\bar{1}$ transition at 200 K is definitely not connected with a BEDT-TTF ordering, the main transformations must take place within the anion layer.

Looking attentively at the 150 K structure projection, presented in Fig. 2, one can notice a visible displacement of both solvent and H_3O molecules from the symmetrical position on the 2-fold axis of the monoclinic phase (shift directions are shown by thick arrows in Fig. 2). In order to estimate and compare the values of atomic shifts in the anion and donor layers, the symmetry of the high-temperature monoclinic state, $C2/c$, was introduced into the low-temperature triclinic structure: as a result the molecules from the adjacent layers of the triclinic phase appeared to be superposed. The derived pictures are presented in Fig. 4. As can be seen, the positions of all components of the complex anion layer differ in two adjacent anion layers (black and white molecules in Fig. 4a). The $[Fe(C_2O_4)_3]^{3-}$ anion moves mainly along a, the solvent displacement occurs within its molecular plane, while H_3O^+ shifts in the perpendicular direction. The magnitude of the atomic displacements reaches 0.55 Å for O atoms of the anion and 1.0 Å for C atoms of the solvent. Owing to the positional shift of a large number of atoms, including Fe, the intensity of the additional peaks which appear under the phase transition is rather high (see Fig. 1b and Fig. 1 in ESI†). The maximum shift is observed for the solvent molecules, *i.e.*, the neutral guest solvent plays a very important role in the phase transition.

The relative displacement of the donors in two independent layers is illustrated in Fig. 4b. The shift of BEDT-TTF molecules is smaller than the displacement of the anion layer constituents and does not exceed 0.15 Å for individual atoms of the TTF core. Hence, at least apparently, the structural transition only weakly affects the BEDT-TTF arrangement inside the conducting layer.

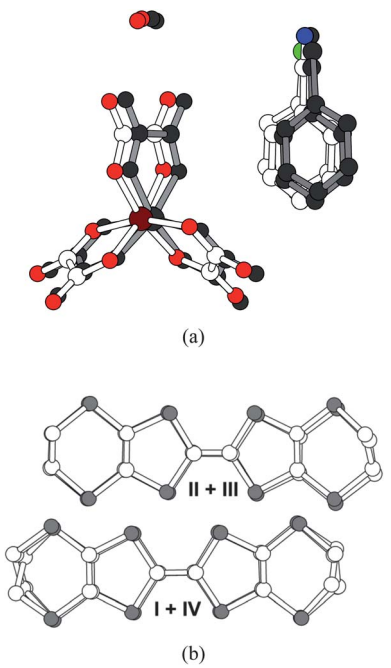

Fig. 4 The relative shift of the molecules resulting from the structural monoclinic to triclinic phase transition in the adjacent anion layers (a) is much larger than in the adjacent donor layers (b). Superposed molecules from different anion layers are shown by white and black colors in (a). H-atoms are omitted for clarity.

Electronic band structure

To have some hint of the consequences of the structural transition for the electronic structure we calculated the $\beta_{HOMO\text{-}HOMO}$ interaction energies[24] for the different donor-donor interactions in the β'' layer of the high temperature monoclinic phase and the two layers of the low temperature triclinic phase. Layers T1 and T2 of the triclinic phase are those containing the I/II and III/IV donors, respectively (see Fig. 2). As shown in Fig. 5, every layer contains two different donors (noted A and B) and the repeat unit contains four donors. There are eight different donor–donor interactions: three of them along the stacks (i to iii), three along the π-stacks (iv to vi) and two along the direction of the step-chains (vii and viii).

The calculated $\beta_{HOMO\text{-}HOMO}$ interaction energies are reported in Table 1. These values clearly show that the differences in the strength of the HOMO–HOMO interactions in the three layers are quite small. In fact, only two of the interactions along the stack, interactions ii (A–A) and iii (B–B), in one of the two layers (T1) of the triclinic phase are a bit stronger. However, these interactions are two of the three weaker HOMO–HOMO interactions and it is not expected that these differences afford any noticeable change in the electronic structure. It must be noted that in the triclinic phase there is some scattering in the central C=C bond lengths; these bond lengths are 1.364(5) and 1.353(5) Å in one layer (T1) but 1.377(5) and 1.375(5) Å in the other (T2) in spite of the same flattened geometry of the TTF-cores in both layers. In the monoclinic phase the two bond lengths are 1.367(3) and 1.371(3) Å. However, the calculated energies of the HOMO for the different donors in the triclinic and monoclinic phases are very similar, all lying in a very narrow energy range of 0.03 eV. Consequently, neither the HOMO energies nor the HOMO–HOMO interactions differ sizably so that it is not expected that the structural transition brings about any noticeable variation in the electronic structure.

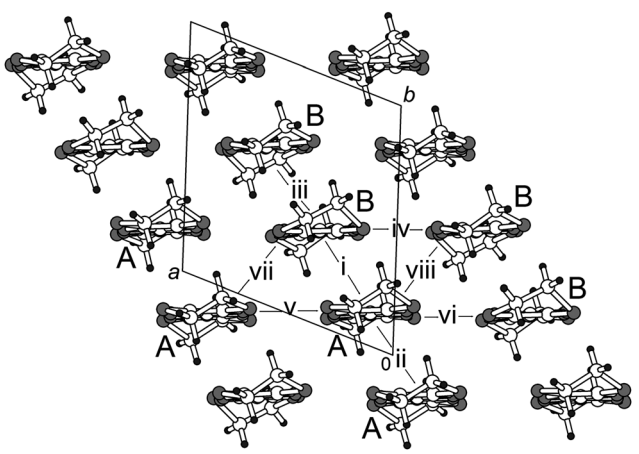

Fig. 5 Donor layer of the β''-type where the different donors (A, B), donor–donor interactions (i to viii) and main axes (a and b) used for the electronic structure calculations are labeled.

Table 1 Calculated values of the $|\beta_{HOMO\text{-}HOMO}|$ (eV) for the different donor···donor interactions of the β″ layer in the monoclinic phase and the two different β″ layers in the triclinic phase of β″-(BEDT-TTF)$_4$H$_3$O[Fe(C$_2$O$_4$)$_3$](BN)$_{0.35}$(CB)$_{0.65}$

Interaction	Monoclinic phase	Triclinic phase (layer T1)[a]	Triclinic phase (layer T2)[b]
i (A–B)	0.2306	0.2334	0.2282
ii (A–A)	0.1059	0.1330	0.1034
iii (B–B)	0.1020	0.1261	0.0949
iv (B–B)	0.1524	0.1572	0.1589
v (A–A)	0.0891	0.0922	0.0924
vi (A–B)	0.1534	0.1650	0.1532
vii (A–B)	0.2523	0.2515	0.2620
viii (A–B)	0.2829	0.2972	0.2833

[a] Layer T1 contains donors I and II (see Fig. 2). [b] Layer T2 contains donors III and IV (see Fig. 2).

To facilitate the comparison, the band structure and Fermi surface for the three different donor layers were calculated using the *a* and *b* axes defined in Fig. 5. With this convention the donor stacks always occur along the diagonal direction. The three calculations led to almost identical results, as expected from the previous analysis. Shown in Fig. 6 are the calculated band structure and Fermi surface for one of the two layers (T1) of the triclinic phase. The four bands of Fig. 6a are mostly built from the HOMO of the four donors. The average charge of the donors is +1/2, so that there must be two holes in these bands. Since the two upper bands overlap, the two bands are partially filled and the system must be metallic in agreement with the transport measurements (see below). The Fermi surface (Fig. 6b) is made of closed pockets of electrons (around the X point) and holes (around the M S^{-1} point) with an area of 7.4% (monoclinic), 8.4% (triclinic, layer T1) and 8.4% (triclinic, layer T2) of the cross section of the Brillouin zone. As analyzed elsewhere, these closed pockets result from the hybridization of superposing ellipses with an area of 100% of the cross section of the Brillouin zone.[25] These Fermi surfaces do not exhibit any nesting property so that it is expected that the metallic state is stable until very low temperatures.

Conductivity

The results of the interlayer resistance measurements on the β″-(BEDT-TTF)$_4$H$_3$O[Fe(C$_2$O$_4$)$_3$](BN)$_{0.35}$(CB)$_{0.65}$ crystal as a function of the temperature are presented in Fig. 7. The sample demonstrates metallic behavior in the whole temperature range down to the superconducting transition which takes place at about 6 K. An interesting feature is observed in the 180–200 K region: one can see the hysteresis in the $R(T)$ dependence when the temperature is sweeping up and down (the insert in Fig. 7). It is worth noting that hysteresis is observed around the temperature at which the structural phase transition takes place.

Conclusion

In conclusion, the structural phase transition from monoclinic $C2/c$ to triclinic $P\bar{1}$ symmetry is discovered at 180–230 K in five organic metals and superconductors of the known β″-(BEDT-TTF)$_4$H$_3$O[Fe(C$_2$O$_4$)$_3$]·G family [G = FB, CB, (BN)$_{0.40}$(FB)$_{0.60}$, (BN)$_{0.35}$(CB)$_{0.65}$, (BN)$_{0.17}$(BB)$_{0.83}$]. Detailed X-ray structural study of the β″-(BEDT-TTF)$_4$H$_3$O[Fe(C$_2$O$_4$)$_3$](BN)$_{0.35}$(CB)$_{0.65}$ crystal shows that the main structural changes consist of strong

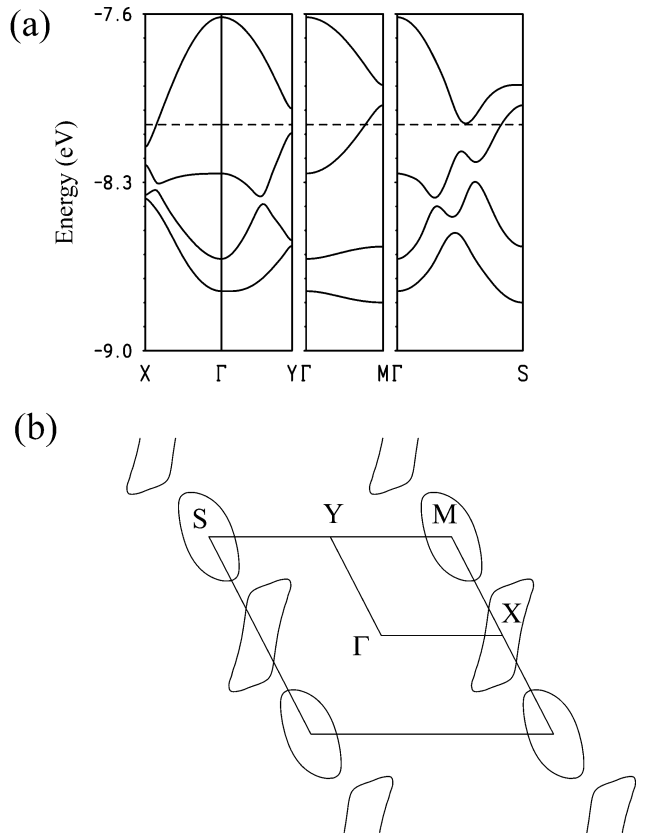

Fig. 6 Calculated band structure (a) and Fermi surface (b) for layer T1 of the triclinic structure of β″-(BEDT-TTF)$_4$H$_3$O[Fe(C$_2$O$_4$)$_3$](BN)$_{0.35}$(CB)$_{0.65}$. The dashed line in (a) refers to the Fermi level. Γ = (0, 0), X = (a*/2, 0), Y = (0, b*/2), M = (a*/2, b*/2) and S = (−a*/2, b*/2) where a and b are the repeat vectors defined in Fig. 5.

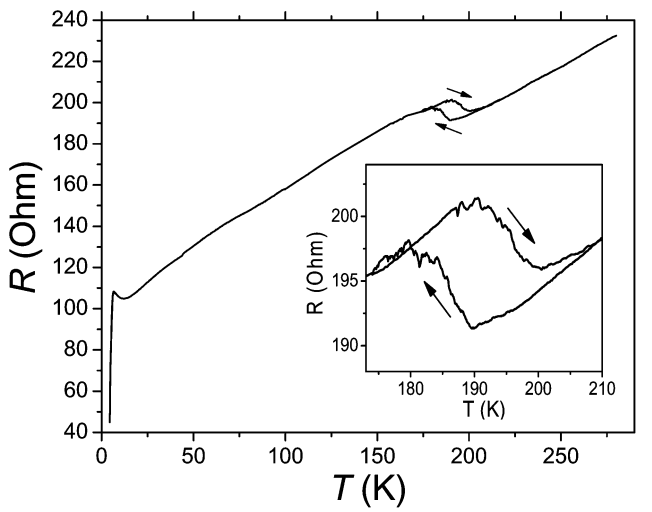

Fig. 7 Interlayer resistance of the superconducting β″-(BEDT-TTF)$_4$H$_3$O[Fe(C$_2$O$_4$)$_3$](BN)$_{0.35}$(CB)$_{0.65}$ crystal ($T_c \approx 6$ K) as a function of temperature. A phase transition with hysteresis in the $R(T)$ dependence shown in the insert is observed around the temperature of the structural phase transition.

positional shifts of the components of the complex anion layer: anions $[Fe^{III}(C_2O_4)_3]^{3-}$, cations H_3O^+ and neutral guest solvents G. The phase transition weakly affects the conducting layer crystal and electronic structure and does not prevent the important process of positional ordering of BEDT-TTF molecules at lower temperature. Because of these reasons the conducting properties of the crystals do not change significantly during the phase transition and the crystals preserve the possibility of entering into a superconducting state. In the $R(T)$ dependence a little jump of the resistivity with hysteresis of about 10 degrees occurs around the temperature of the structural transformation. The presence of hysteresis is an indication of a first order phase transition.

Acknowledgements

This work was partially supported by the RFBR grants 09-02-00241, 09-02-00852 and the Russian Government contract No. 14.740.11.0911. Work at Bellaterra was supported by DGES-Spain (Projects FIS2009-12721-C04-03 and CSD2007-00041).

References

1 T. G. Prokhorova, L. I. Buravov, E. B. Yagubskii, L. V. Zorina, S. S. Khasanov, S. V. Simonov, R. P. Shibaeva, A. V. Korobenko and V. N. Zverev, *CrystEngComm*, 2011, **13**, 537.
2 M. Kurmoo, A. W. Graham, P. Day, S. J. Coles, M. B. Hursthouse, J. L. Caufield, J. Singleton, F. L. Pratt, W. Hayes, L. Ducasse and P. Guionneau, *J. Am. Chem. Soc.*, 1995, **117**, 12209.
3 H. Akutsu, A. Akutsu-Sato, S. S. Turner, P. Day, E. Canadell, S. Firth, R. J. N. Clark, J. Yamada and S. Nakatsuji, *Chem. Commun.*, 2004, 18.
4 L. Martin, P. Day, H. Akutsu, J. Yamada, S. Nakatsuji, W. Clegg, R. W. Harrington, P. N. Horton, M. B. Hursthouse, P. McMillan and S. Firth, *CrystEngComm*, 2007, **9**, 865.
5 L. Martin, S. S. Turner, P. Day, F. E. Mabbs and J. L. McInnes, *Chem. Commun.*, 1997, 1367.
6 L. Martin, S. S. Turner, P. Day, P. Guionneau, J. A. K. Howard, D. E. Hibbs, M. E. Light, M. B. Hursthouse, M. Uruichi and K. Yakushi, *Inorg. Chem.*, 2001, **40**, 1363.
7 S. Rashid, S. S. Turner, P. Day, J. A. K. Howard, P. Guionneau, E. J. L. McInnes, F. E. Mabbs, R. J. H. Clark, S. Firth and T. Biggse, *J. Mater. Chem.*, 2001, **11**, 2095.
8 A. Audouard, V. N. Laukhin, L. Brossard, T. G. Prokhorova, E. B. Yagubskii and E. Canadell, *Phys. Rev. B: Condens. Matter Mater. Phys.*, 2004, **69**, 144523.
9 E. Coronado, S. Curelli, C. Giménez-Saiz and C. J. Gómez-García, *Synth. Met.*, 2005, **154**, 245.
10 L. V. Zorina, S. S. Khasanov, S. V. Simonov, R. P. Shibaeva, V. N. Zverev, E. Canadell, T. G. Prokhorova and E. B. Yagubskii, *CrystEngComm*, 2011, **13**, 2430.
11 S. S. Turner, P. Day, K. M. Abdul Malik, M. B. Hursthouse, S. J. Teat, E. J. MacLean, L. Martin and S. A. French, *Inorg. Chem.*, 1999, **38**, 3543.
12 S. Rashid, S. S. Turner, D. Le Pevelen, P. Day, M. E. Light, M. B. Hursthouse, S. Firth and R. J. H. Clark, *Inorg. Chem.*, 2001, **40**, 5304.
13 T. G. Prokhorova, S. S. Khasanov, L. V. Zorina, L. I. Buravov, V. A. Tkacheva, A. A. Baskakov, R. B. Morgunov, M. Gener, E. Canadell, R. P. Shibaeva and E. B. Yagubskii, *Adv. Funct. Mater.*, 2003, **13**, 403.
14 L. V. Zorina, T. G. Prokhorova, S. V. Simonov, S. S. Khasanov, R. P. Shibaeva, A. I. Manakov, V. N. Zverev, L. I. Buravov and E. B. Yagubskii, *J. Exp. Theor. Phys.*, 2008, **106**, 347.
15 A. I. Coldea, A. F. Bangura, J. Singleton, A. Ardavan, A. Akutsu-Sato, H. Akutsu, S. S. Turner and P. Day, *Phys. Rev. B: Condens. Matter Mater. Phys.*, 2004, **69**, 085112.
16 A. I. Coldea, A. F. Bangura, J. Singleton, A. Ardavan, A. Akutsu-Sato, H. Akutsu and P. Day, *J. Low Temp. Phys.*, 2006, **142**, 253.
17 A. Akutsu-Sato, H. Akutsu, J. Yamada, S. Nakatsuji, S. S. Turner and P. Day, *J. Mater. Chem.*, 2007, **17**, 2497.
18 E. Coronado, S. Curelli, C. Giménez-Saiz and C. J. Gómez-García, *J. Mater. Chem.*, 2005, **15**, 1429.
19 Oxford Diffraction (2007). Oxford Diffraction Ltd., *Xcalibur CCD system, CrysAlisPro Software system, Version 1.171.32*.
20 G. M. Sheldrick, *Acta Crystallogr., Sect. A: Found. Crystallogr.*, 2008, **64**, 112.
21 M.-H. Whangbo and R. Hoffmann, *J. Am. Chem. Soc.*, 1978, **100**, 6093.
22 J. H. Ammeter, H.-B. Bürgi, J. Thibeault and R. Hoffmann, *J. Am. Chem. Soc.*, 1978, **100**, 3686.
23 A. Pénicaud, K. Boubekeur, P. Batail, E. Canadell, P. Auban-Senzier and D. Jérome, *J. Am. Chem. Soc.*, 1993, **115**, 4101.
24 M.-H. Whangbo, J. M. Williams, P. C. W. Leung, M. A. Beno, T. J. Emge and H. H. Wang, *Inorg. Chem.*, 1985, **24**, 3500.
25 R. Rousseau, M. Gener and E. Canadell, *Adv. Funct. Mater.*, 2004, **14**, 201.